Electronic Supplementary Material (ESI) for Journal of Materials Chemistry C.

Integrating TADF Luminogens with AIE Characteristics Using Novel Acridine-Carbazole Hybrid as Donor for High-Performance and Low Efficiency Roll-off OLEDs

Qing Zhang, Shuaiqiang Sun, Wei Liu, Panpan Leng, Xialei Lv, Yaxiong Wang, Hongting Chen, Shaofeng Ye, Shaoqing Zhuang, Lei Wang *

Wuhan National Laboratory for Optoelectronics, Huazhong University of Science and Technology, Wuhan, 430074, P. R. China

*Email: wanglei@mail.hust.edu.cn

The computational details, measurement instruments, device fabrication and measurement cited our previous reports.[1-3] The evaluation of exciton dynamic rate constants was calculated by equation S1-S7.[4] The prerequisites for establishment of Equation S3 is the non-radiative rate constants of the triplet state (k_{nr}^{T}=0) are significantly lower than k_{RISC} when T_1 is relatively stable, the quantum yield of the reverse intersystem crossing is almost 100% (Φ_{RISC} = 1).[4, 5]

$$k_{PF} = \frac{\phi_{PF}}{\tau_P} \quad \text{Equation S1}$$

$$k_{DF} = \frac{\phi_{DF}}{\tau_D} \quad \text{Equation S2}$$

$$k_{ISC} = \frac{\phi_{DF}}{\phi_{PF}+\phi_{DF}} k_{PF} \quad \text{Equation S3}$$

$$k_{RISC} = \frac{k_{DF}k_{PF}}{k_{ISC}} \frac{\phi_{DF}}{\phi_{PF}} \quad \text{Equation S4}$$

$$k_{PF} = k_r^S + k_{nr}^S + k_{ISC} \quad \text{Equation S5}$$

$$\phi_{PF} = \frac{k_r^S}{k_r^S+k_{nr}^S+k_{ISC}} = \frac{k_r^S}{k_{PF}} \quad \text{Equation S6}$$

$$\phi_{ISC} = \frac{k_{ISC}}{k_r^S+k_{nr}^S+k_{ISC}} = \frac{k_{ISC}}{k_{PF}} \quad \text{Equation S7}$$

Table S1 The detail kinetic parameters

Compounds	ϕ_{PL} [a] (%)	ϕ_P/ϕ_D [b] (%)	τ_p/τ_d [c] (ns)/(μs)	k_{PF} [d] (10^6 s^{-1})	k_{DF} [d] (10^5 s^{-1})	k_{ISC} [d] (10^6 s^{-1})	k_{RISC} [d] (10^5 s^{-1})	k^S_r [d] (10^6 s^{-1})	k^S_{nr} [d] (10^5 s^{-1})	Φ_{ISC} [d] (%)
34AcCz-PM [e]	88	39/49	67/0.73	5.76	6.72	3.22	15.27	2.23	3.04	56
34AcCz-Trz [e]	69	39/30	73/0.88	5.40	3.37	2.32	5.92	2.12	9.54	43
34AcCz-PM [f]	67	36/31	81/0.64	4.47	4.85	2.06	8.97	1.62	7.96	46
34AcCz-Trz [f]	42	26/16	55/0.75	4.72	2.13	1.79	1.79	1.23	16.98	38

[a] Absolute PL quantum yield measured with integrating spheres, [b] calculated by integral area of Fig 4b; [c] Fitted from Fig 4b and Fig S3b; [d] calculated using equations S1-S7. [e] *wt*% dopant in CBP films (*x wt*% dopant: *x*=10 for **34AcCz-PM**; *x*=5 for **34AcCz-Trz**). [f] neat film.

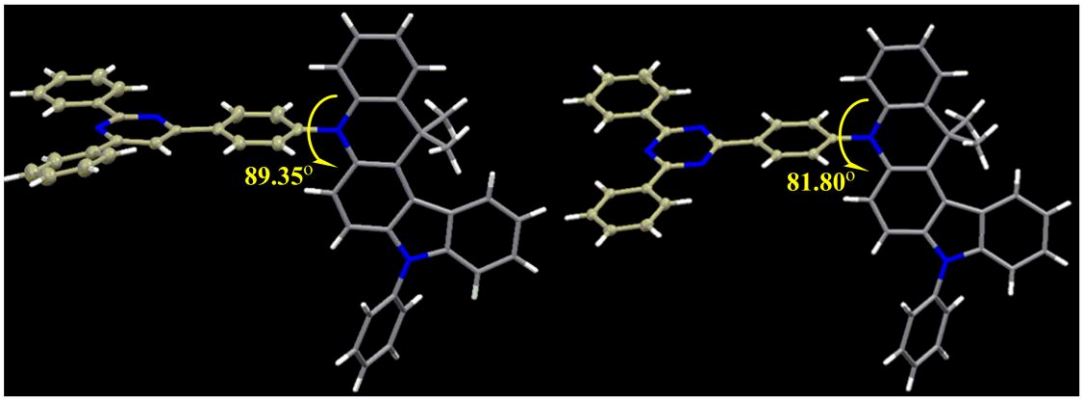

Fig S1. Crystal structures of (CCDC 1877512) and (right) **34AcCz-Trz** (1877513)

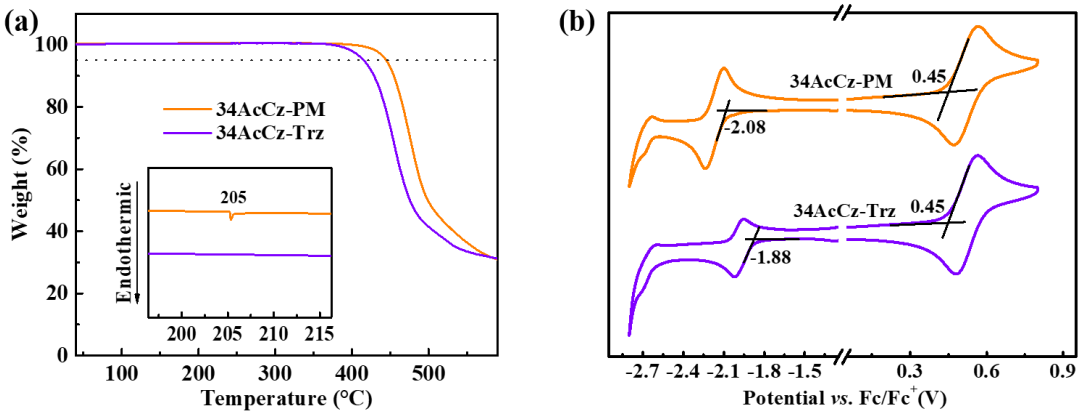

Fig S2. (a) Thermal thermograms (TGA and DSC thermograms) and (b) Cyclic voltammogram of **34AcCz-PM** and **34AcCz-Trz**.

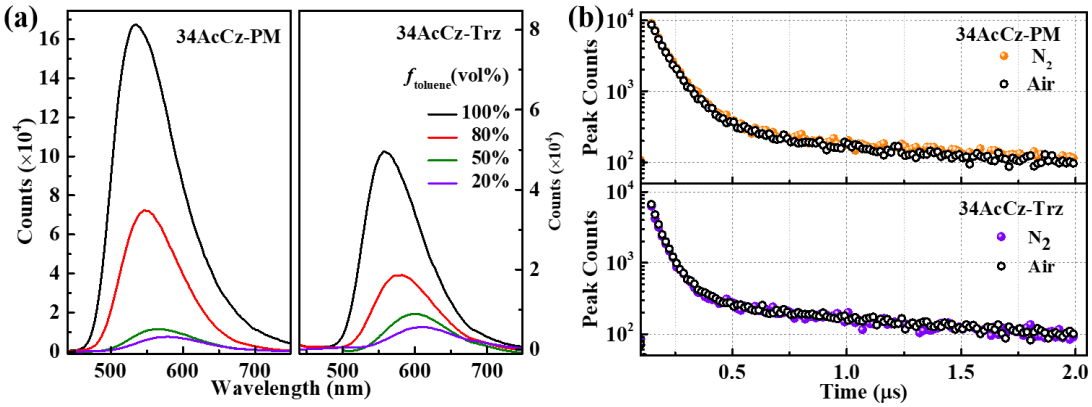

Fig S3. (a) PL spectra of **34AcCz-PM** and **34AcCz-Trz** in THF/Toluene mixtures with different toluene fractions ($f_{toluene}$ (vol)) (b) PL decay spectra of pure films of **34AcCz-PM** and **34AcCz-Trz**.

Scheme S1 The details of device structure, chemical structures of materials, the related description and fitting mode.

Device A: MoO_3 (10)/ TAPC (100)/ TCTA (5)/ CBP: 10% **34AcCz-PM** (20)/ TmPyPB (40)/ LiF (1)/ Al	
Device B: MoO_3 (10)/ TAPC (80)/ TCTA (5)/ CBP: 5% **34AcCz-Trz** (25)/ TmPyPB (40)/ LiF (1)/ Al	
Device C: MoO_3 (10)/ TAPC (45)/ TCTA(5)/ **34AcCz-PM** (15)/ TmPyPB (30)/ LiF (1)/ Al	
Device D: MoO_3 (10)/ TAPC (80)/ TCTA (5)/ **34AcCz-Trz** (10)/ TmPyPB (50)/ LiF (1)/Al	
34AcCZ-PM	Hole-only: ITO/ MoO_3 (10)/ TAPC (100)/ TCTA (5)/ CBP: *x*% **34AcCz-PM** (20)/TCTA (5)/TAPC (100)/MoO_3. Electron-only: ITO/ LiF (1)/ TmPyPB (40)/ CBP: *x*% **34AcCz-PM** (20)/ TmPyPB (40)/ LiF (1)/Al.
34AcCZ-Trz	Hole-only: ITO/ MoO_3 (10)/ TAPC (80)/ TCTA (5)/ CBP: *x*% **34AcCz-Trz** (25)/ TCTA (5)/ TAPC (80)/ MoO_3 (10)/Al. Electron-only: ITO/ LiF (1)/ TmPyPB (40)/ CBP: *x*% **34AcCz-Trz** (25)/TmPyPB (40)/ LiF (1)/ Al.

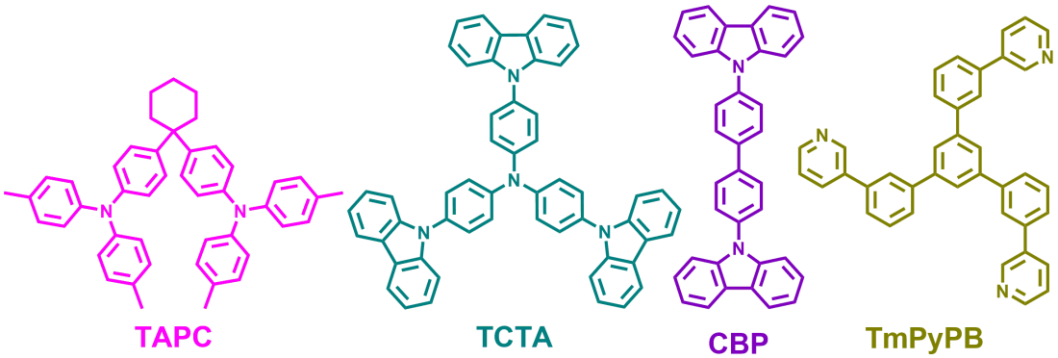

MoO_3 and LiF acted as hole- and electron-injecting layers, respectively. TAPC (1,1-bis[4-[*N*,*N*-di(*p*-tolyl)-amino]phenyl]-cyclohexane) and TmPyPB (1,3,5-tri(*m*-pyrid-3-yl-phenyl) benzene) were served as the hole- and electron-transporting layers, respectively. The thin layer of TCTA (tris(4-(9*H*-carbazol-9-yl)phenyl)amine) was incorporated as an exciton blocking layer. CBP (4,4'-di(9*H*-carbazol-9-yl)-1,10-

biphenyl was used as host.

The TTA mode simulation can be described as follow:[6-8]

$$\frac{\eta}{\eta_0} = \frac{J_0}{4J}\left(\sqrt{1+8\frac{J}{J_0}} - 1\right) \qquad \text{Equation S9}$$

where η, η_0, and J_0 represent the *EQE* of the device *EQE*, initial *EQE* in the absence of TTA, and the current density at the half-maximum of the EQE, respectively.

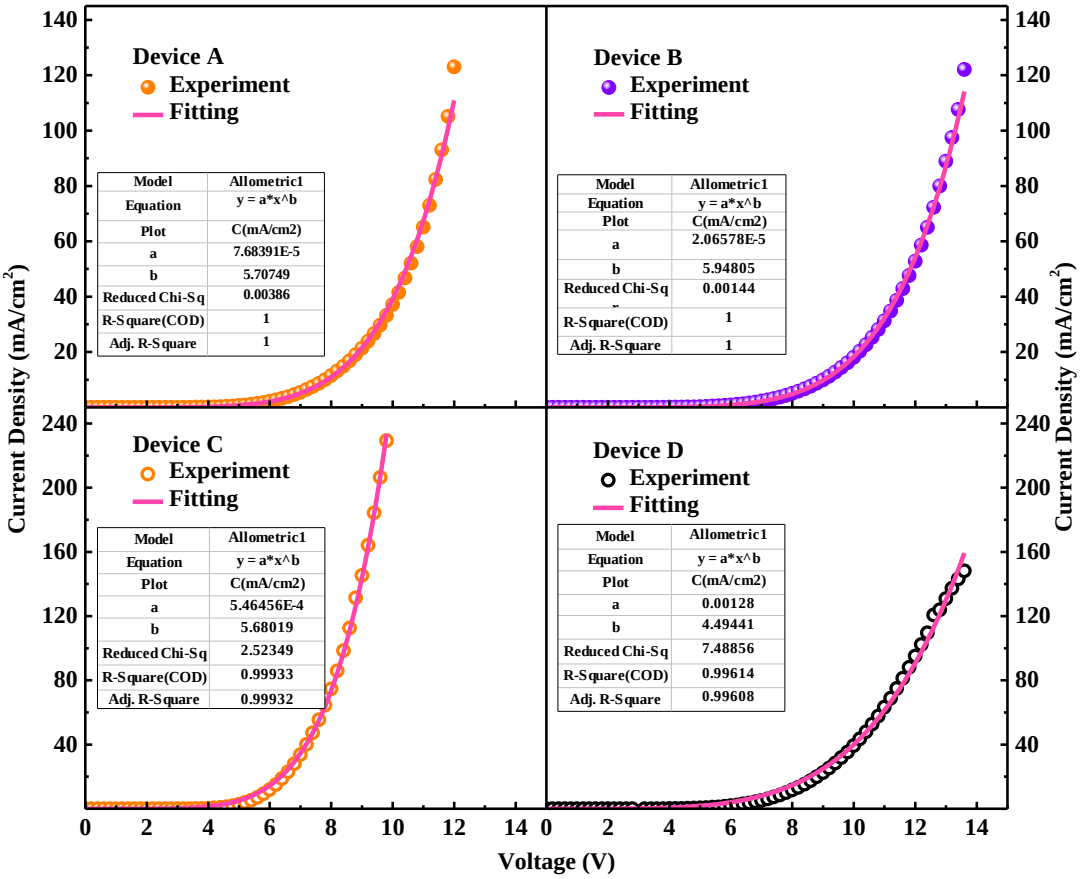

Fig S4. Current density-voltage curves of the devices and the fitting results according to $J \propto V^{l+1}$equation.

Assuming bulk limited transport (**Fig. S4**), the equation for TPQ model can be expressed as follows:[6, 9]

$$\frac{\eta}{\eta_0} = \frac{1}{1+CJ^{\frac{1}{l+1}}} \qquad \text{Equation S10}$$

where η_0 is the device EQE in the absence of TPQ, J stands for the current density of the device, and C is a constant which is related to the parameters like dielectric constant, carrier mobility, TPQ rate constant and decay lifetime of system. According to the previous work, l in Equation S10 needs to be an integer greater than 1 to make this equation reasonable.

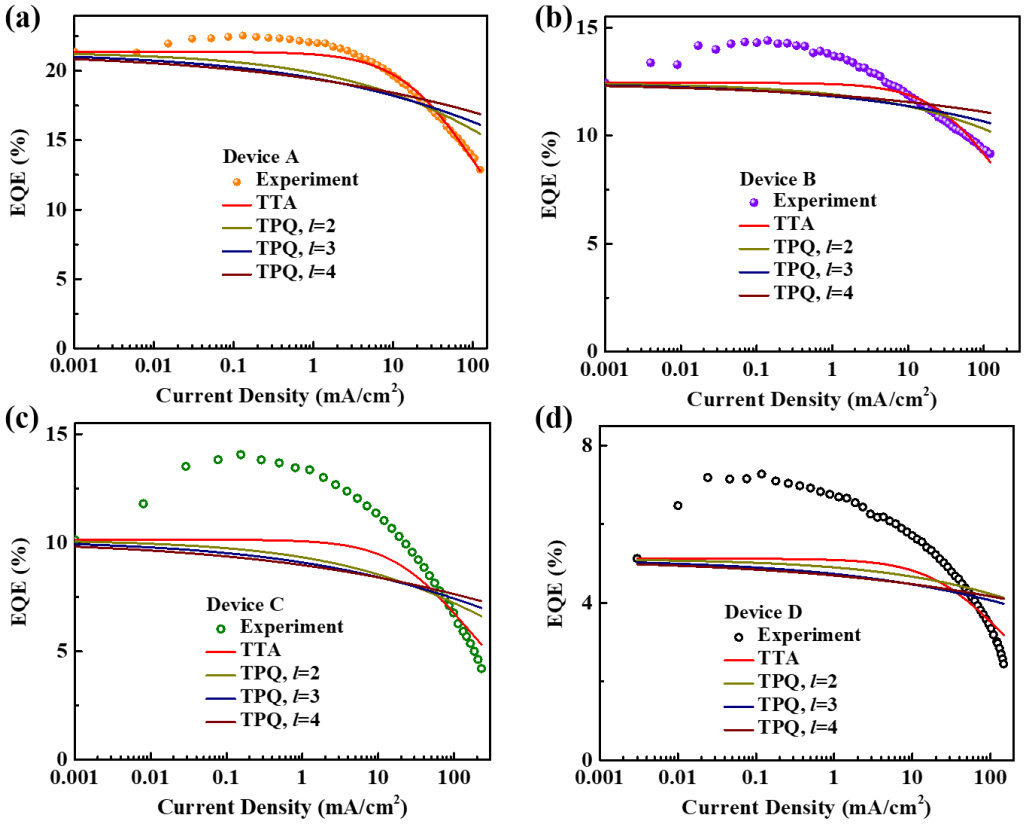

Fig S5. The external quantum efficiency (EQE) as a function of current density and the fitting results according to triplet–triplet annihilation (TTA) and triplet-polaron quenching (TPQ) mechanism.

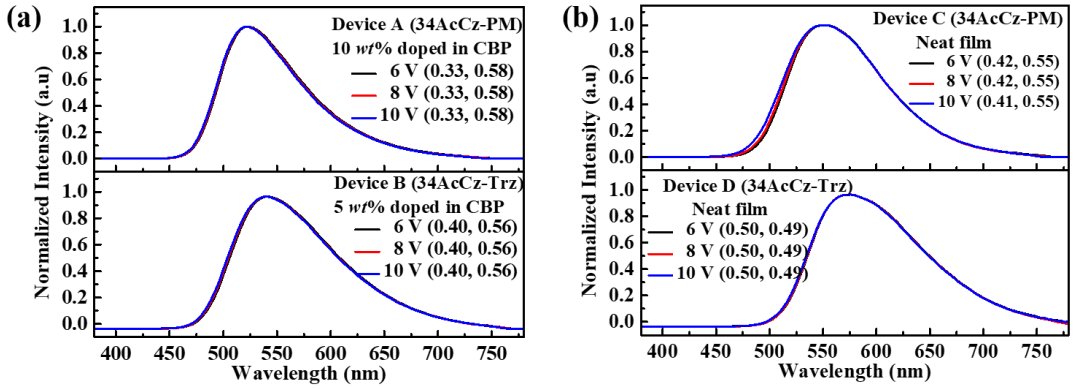

Fig S6. EL spectra and color gamuts of device A-D measured at different voltages, respectively.

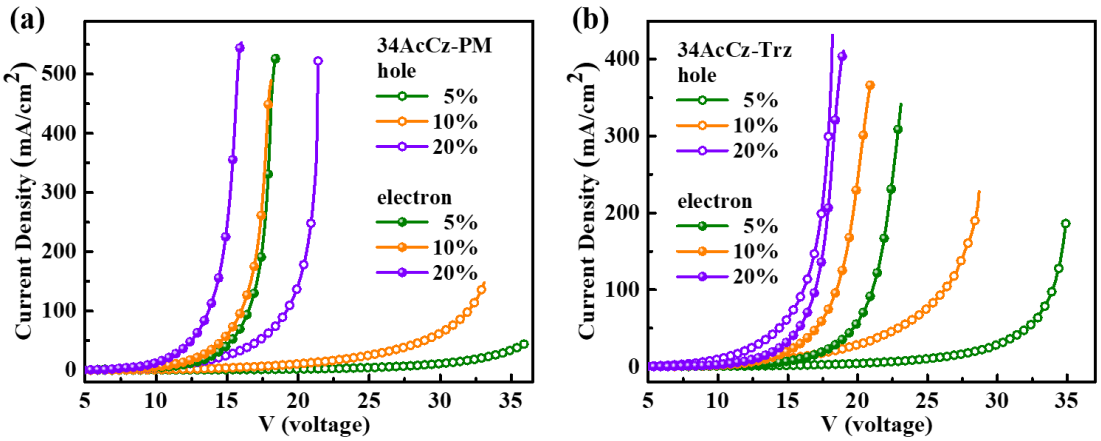

Fig S7. Current density-voltage characteristics of hole-only and electron-only devices with different concentrations for (a) **34AcCz-PM** and (b) **34AcCz-Trz**.

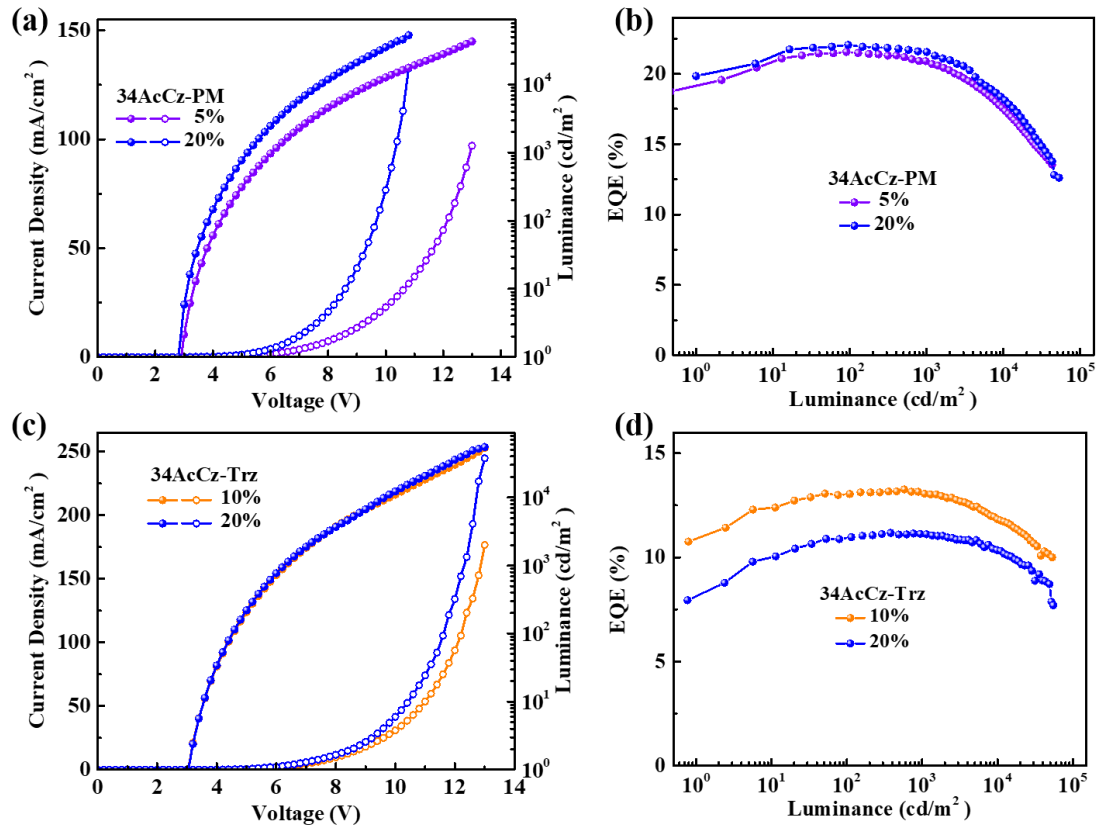

Fig S8. Current density–voltage–luminance (*C–V–L*) curves and EQE as a function of the luminance for **34AcCz-PM** (a) and (b) (5 *wt*% and 20 *wt*%); **34AcCz-Trz** (c) and (d) (10 *wt*% and 20 *wt*%). (Note: The device structure were referenced to the optimal structure; 5 *wt*% is the lowest dopant concentration that we can fabricate for this material system.)

Table S2. EL performances the doped devices with different dopant concentration.

Emitter [a]	V_{on} [b]	η_{max} [c]	CE [d]	PE [d]	EQE [d]	$CIE_{x,y}$ [e]	λ [f]
34AcCz-PM (5%)	2.85	70.9/ 66.2/ 21.6	68.6/ 62.1	35.6/ 23.8	20.8/ 18.9	(0.32,0.59)	524
34AcCz-PM (20%)	2.80	70.1/ 70.4/ 22.0	69.0/ 62.0	41.6/ 28.0	21.5/ 19.3	(0.34,0.57)	520
34AcCz-Trz (10%)	3.15	39.6/ 33.3/ 13.3	39.3/ 37.5	19.5/ 13.9	13.1/ 12.4	(0.43,0.54)	548
34AcCz-Trz (20%)	3.14	32.1/ 25.3/ 11.2	31.9/ 31.3	16.0/ 11.5	11.1/ 10.8	(0.40,0.56)	540

Table S3. EL performances of nodoped devices based on AIE-TADF emitters.

Emitter [a]	V_{on} [b]	η_{max} [c]	CE [d]	PE [d]	EQE [d]	$CIE_{x,y}$ [e]	λ [f]	Referenc
34AcCz-PM	3.10	45.2/40.0/14.1	41.2/ 36.0	26.1/ 17.8	12.8/ 10.7	(0.42, 0.55)	548	**This work**
34AcCz-Trz	3.35	18.0/15.5/ 7.3	14.6/ 11.5	6.3/ 4.0	5.9/ 4.5	(0.50, 0.49)	576	**This work**
mSOAD	3.1	31.7/28.4/14.0	—	—	—	(0.18, 0.32)	480	10
PXZ2PTO	4.3	44.9/32.0/16.4	29.0/ —	8.9/ —	10.4/ —	(0.27,0.50)	504	11
DBT-BZ-DMAC	2.7	43.3/35.7/14.2	43.1/ —	33.1/ —	14.2/ —	(0.26, 0.55)	—	12
DCPDAPM	3.2	26.9/15.6/ 8.2	21.4/ —	15.3/ —	6.5/ —	(0.26, 0.56)	522	13
4,4-CzSPz	3.6	61.2/ 38.4/ 20.7	30.2/ —	16.0/ —	10.3/ —	—	526	14
CCDD	2.4	39.8/41.7/12.7	—	—	8.8/ —	(0.39, 0.56)	543	15
DCB-BP-PXZ	2.5	72.9/ 81.8/ 22.6	—/ 64.6	—/ 60.8	—/ 20.1	(0.39, 0.57)	548	16
*m*CBP-BP-PXZ	2.5	70.4/ 76.5/ 21.8	—/ 63.4	—/ 47.5	—/ 19.6	(0.38, 0.57)	542	16
SBDBQ-DMAC	2.8	35.4/ 32.7/ 10.1	21.2/ —	10.7/ —	6.0/ —	(0.39, 0.58)	544	17
DBQ-3DMAC	2.6	41.2/ 45.4/ 12.0	28.5/ —	17.6/ —	8.3/ —	(0.40, 0.57)	548	17
CP-BP-PXZ	2.5	59.1/ 65.7/ 18.4	58.4/ —	49.7/ —	18.2/ —	(0.40, 0.57)	548	18
CP-BP-PTZ	2.5	46.1/ 55.7/ 15.3	38.4/ —	30.2/ —	12.7/ —	(0.42, 0.55)	554	18
DBT-BZ-PXZ	2.9	26.6/ 27.9/ 9.2	19.6/ —	11.3/ —	6.8/ —	(0.43, 0.54)	557	19
DBT-BZ-PTZ	2.7	26.5/ 29.1/ 9.7	23.5/ —	15.4/ —	8.5/ —	(0.45, 0.53)	563	19
DPF-BP-PXZ	2.6	41.6/ 45.0/ 14.3	41.4/ —	26.0/ —	14.1/ —	(0.46, 0.53)	—	20
SBF-BP-PXZ	2.5	36.8/ 37.9/ 12.3	36.7/ —	28.8/ —	12.2/ —	(0.46, 0.53)	—	20
PTZ-XT	3.0	—/ —/ 11.1	—	—	—	—	553	21
PTZ-BP	3.0	—/ —/ 7.6	—	—	—	—	577	21
SFDBQPXZ	3.4	24.3/22.5/ 10.1	14.2/– –	6.3/ —	6.0/ —	—	584	22
DFDBQPXZ	3.2	21.0/20.6/ 9.8	9.8/ —	4.2/ —	4.7/ —	—	588	22
DBQPXZ	3.4	24.9/19.6/ 8.8	17.8/ —	8.3/ —	6.3/ —	—	564	22
2PCZ-CB	4.4	19.9/11.2/ 9.2	—	—	—	—	590	23
PCZ-CB-TRZ	6.3	16.7/7.6/ 11.0	—	—	—	—	586	23
TPA-CB-TRZ	4.4	12.0/7.9/ 10.1	—	—	—	—	631	23

[a] Emitters with AIE and TADF characteristics; [b] Turn-on voltage (at a brightness of 1 cd m^{-2}); [c] The maximum efficiencies of CE (cd A^{-1}), PE (lm W^{-1}) and EQE (%); [d] at 1000 and 5000 cd m^{-2}; [e] Commission International de I'Eclairage coordinates recorded at 8 V; [f] EL peak wavelength (nm).

References

1 Q. Zhang, S. Sun, X. Lv, W. Liu, H. Zeng, R. Guo, S. Ye, P. Leng, S. Xiang and L. Wang, *Mater. Chem. Front.*, 2018, **2**, 2054-2062.

2 X. Lv, W. Zhang, D. Ding, C. Han, Z. Huang, S. Xiang, Q. Zhang, H. Xu and L. Wang, *Adv. Opt. Mater.*, 2018, **6**, 1800165.

3 S. Xiang, X. Lv, S. Sun, Q. Zhang, Z. Huang, R. Guo, H. Gu, S. Liu and L. Wang, *J. Mater. Chem. C*, 2018, **6**, 5812-5820.

4 Y. Tao, K. Yuan, T. Chen, P. Xu, H. Li, R. Chen, C. Zheng, L. Zhang and W. Huang, *Adv. Mater.*, 2014, **26**, 7931-7958.

5 C. Li, C. Duan, C. Han and H. Xu, *Adv. Mater.*, 2018, **30**, e1804228.

6 M. A. Baldo, C. Adachi and S. R. Forrest, *Phys. Rev. B*, 2000, **62**, 10967-10977.

7 S. Reineke, K. Walzer and K. Leo, *Phys. Rev. B*, 2007, **75**.

8 Y.-K. Wang, S.-H. Li, S.-F. Wu, C.-C. Huang, S. Kumar, Z.-Q. Jiang, M.-K. Fung and L.-S. Liao, *Adv. Funct. Mater.*, 2018, **28**, 1706228.

9 Y. Xiang, Z.-L. Zhu, D. Xie, S. Gong, K. Wu, G. Xie, C.-S. Lee and C. Yang, *J. Mater. Chem. C*, 2018, **6**, 7111-7118.

10 J. Li, R. Zhang, Z. Wang, B. Zhao, J. Xie, F. Zhang, H. Wang and K. Guo, *Adv. Opt. Mater.*, 2018, **6**, 1701256.

11 S. Xiang, Z. Huang, S. Sun, X. Lv, L. Fan, S. Ye, H. Chen, R. Guo and L. Wang, *J. Mater. Chem. C*, 2018, **6**, 11436-11443.

12 J. Guo, X.-L. Li, H. Nie, W. Luo, S. Gan, S. Hu, R. Hu, A. Qin, Z. Zhao, S.-J. Su and B. Z. Tang, *Adv. Funct. Mater.*, 2017, **27**, 1606458.

13 Y. Zhao, W. Wang, C. Gui, L. Fang, X. Zhang, S. Wang, S. Chen, H. Shi and B. Z. Tang, *J. Mater. Chem. C*, 2018, **6**, 2873-2881.

14 J. Zhao, X. Chen, Z. Yang, T. Liu, Z. Yang, Y. Zhang, J. Xu and Z. Chi, *J. Phys. Chem. C*, 2018, **123**, 1015-1020.

15 H. Zhao, Z. Wang, X. Cai, K. Liu, Z. He, X. Liu, Y. Cao and S.-J. Su, *Mater. Chem. Front.*, 2017, **1**, 2039-2046.

16 H. Liu, J. Zeng, J. Guo, H. Nie, Z. Zhao and B. Z. Tang, *Angew. Chem. Int. Ed. Engl.*, 2018, **57**, 9290-9294.

17 L. Yu, Z. Wu, G. Xie, W. Zeng, D. Ma and C. Yang, *Chem. Sci.*, 2018, **9**, 1385-1391.

18 J. Huang, H. Nie, J. Zeng, Z. Zhuang, S. Gan, Y. Cai, J. Guo, S.-J. Su, Z. Zhao and B. Z. Tang, *Angew. Chem. Int. Ed. Engl.*, 2017, **56**, 12971-12976.

19 J. Guo, X.-L. Li, H. Nie, W. Luo, R. Hu, A. Qin, Z. Zhao, S.-J. Su and B. Z. Tang, *Chem. Mater.*, 2017, **29**, 3623-3631.

20 J. Guo, J. Fan, L. Lin, J. Zeng, H. Liu, C.-K. Wang, Z. Zhao and B. Z. Tang, *Adv. Sci.*, 2018, **0**, 1801629.

21 N. Aizawa, C.-J. Tsou, I. S. Park and T. Yasuda, *Polym. J.*, 2016, **49**, 197.

22 L. Yu, Z. Wu, G. Xie, C. Zhong, Z. Zhu, D. Ma and C. Yang, *Chem. Commun.*, 2018, **54**, 1379-1382.

23 R. Furue, T. Nishimoto, I. S. Park, J. Lee and T. Yasuda, *Angew. Chem. Int. Ed. Engl.*, 2016, **55**, 7171-7175.